

# Bi-State Frequency Selective Surfaces Made of Intertwined Slot Arrays

Andrea Vallecchi, Richard J. Langley, *Senior Member, IEEE*, and Alexander G. Schuchinsky, *Fellow, IEEE*

**Abstract**— Novel arrangements of active frequency selective surfaces (AFSSs) with integrated voltage control wiring are proposed for bi-state (transparency/reflectance) operation at specified frequencies. The AFSSs are comprised of passive arrays of intertwined patterns of slots in a conductor screen and an active dipole array with *pin* diodes placed either on the same or opposite sides of a thin dielectric substrate. **Simulation and measurement results show that such AFSSs exhibit good isolation ( $\sim 15$  dB) between the translucency and reflection states at normal incidence that slightly decreases at oblique incidence. The proposed AFSSs maintain the high angular and polarisation stability over broad fractional bandwidths (FBWs) inherent to the constituent periodic arrays of intertwined conductor patterns with substantially subwavelength unit cells. The merits of these AFSS arrangements also include resilience to parasitic effects of real switches, whose insertion loss in the *on*-state only enhances the AFSS *on/off* isolation.** Such AFSSs are essential elements for reconfiguring and controlling the electromagnetic architecture of buildings.

**Index Terms**—Periodic structures, active frequency selective surfaces, *pin* diodes, convoluted conductor pattern, subwavelength resonance.

## I. INTRODUCTION

Convoluted and intertwined conductor patterns of frequency selective surfaces (FSSs) enable significant reductions of the unit cell electrical size and broadening fractional bandwidth (FBW) at low resonance frequencies [1]–[4]. Periodic arrays with subwavelength unit cells exhibit high angular and polarisation stability and resilience to the higher order diffraction effects. These properties are instrumental for the design of conformal FSSs and FSSs integrated in small mobile terminals, RF front-ends and other devices where a large number of unit cells is necessary for an efficient interaction of the array with the incident field [5]. Such FSSs are also vitally important for controlling the electromagnetic architecture, spectral efficiency and security of buildings where the feature size of building interiors and office rooms is commensurate with wavelengths in the frequency bands designated for indoor communications. Owing to the complexity of multipath propagation in the built environment, electromagnetic waves

with diverse polarisations can impinge on FSSs at any angles after multiple reflections and scattering [6]. Therefore, walls controlling interference and providing shielding in the buildings require FSSs with a stable frequency and polarisation response across a wide range of incidence angles.

The dynamic use of the electromagnetic spectrum, which is now becoming increasingly widespread, poses new challenges in FSS design. In particular, agile FSSs are needed to meet the requirements of time variable and frequency dependent propagation conditions. While several methods can be employed to control the response of an FSS (see a recent review of reconfigurable metasurfaces and metamaterials in [7]), a common and cost-effective approach is based on incorporating active components into the patterned metallic screen to vary the reactance of the resonant elements [8]. Namely, semiconductor switches, such as *pin* diodes, have been widely used to realize bi-state operation of active FSSs (AFSSs) comprised of dipoles and other resonant elements [9]–[14]. Recently, bi-state switchable AFSSs based on the periodic arrays of interwoven planar spirals with integrated *pin* diodes have been proposed for both single and dual polarisation operation [15], [16]. The distinctive feature of such arrangements is that the spiral conductors of the AFSS constituent elements also serve as the path for supplying dc bias to *pin* diodes thus eliminating the need of dedicated wiring which may severely distort the RF response. This approach also dramatically simplifies the AFSS topology without compromising the FSS performance.

In this work we present novel architectures of reconfigurable bi-state AFSSs based on the complementary layout of the interwoven spiral [3], [4] and Brigid's cross arrays [17], [18]. The AFSSs contain a patterned conductor sheet with a periodic array of intertwined slots located on one side of a thin dielectric substrate. The *pin* diodes and the strips supplying the dc bias form an active dipole array which is deployed either on the other side of the dielectric substrate or interspersed between the slot array elements in a single layer AFSS configuration. The two patterned conductors are insulated from each other in both configurations. The proposed arrangements combine the merits of passive FSSs with substantially subwavelength unit cells and grids of active dipoles with embedded *pin* diodes. The

Manuscript received August 2016,.... This work was supported by the European Commission 7<sup>th</sup> Framework Program Marie Curie IAPP project grant no. 286333, "WiFEEB—Wireless Friendly Energy Efficient Buildings".

A. Vallecchi is with the Department of Engineering Science, University of Oxford, Oxford OX1 3PJ, UK, on leave from the Department of Electronic and Electrical Engineering, University of Sheffield, Sheffield, UK.

R. J. Langley is with the Department of Electronic and Electrical Engineering, University of Sheffield, Sheffield S1 3JD, U.K. (r.j.langley@sheffield.ac.uk).

A. G. Schuchinsky is with Dept. of Electrical Engineering and Electronics, University of Liverpool, Liverpool L69 3BX, UK (e-mail: A.Schuchinsky@liverpool.ac.uk).

switchable grid has negligible effect on the passband resonance of the slot array in one state of the diodes but acts as a reflective surface in the other one. It also allows independent control of the transmission responses at both the vertical and horizontal polarizations. Such AFSSs maintain the virtues of the passive interwoven arrays while being essentially immune to parasitic effects of switches. An important advantage of the proposed AFSSs is that they are manufacturable by standard low cost PCB photolithography or inkjet printing combined with surface mount technology (SMT) for automated component placement into the planar AFSS conductor patterns.

The objective of this work was to explore the feasibility of using interwoven conductor patterns in switchable AFSS. While our aim here is to demonstrate and prove the concept, the issues of designing a smart wall for a given specification have been addressed in earlier publications. In particular, a convenient and energy efficient way to realize an active wall for controlling the propagation environment is provided by the concept of “Intelligent walls” (IW), originally proposed in [19], [20]. According to the IW approach, when large cross-sectional area within building needs to be electromagnetically isolated or vice-versa using AFSSs, instead of deploying the AFSS over the entire wall, which would be costly and energy inefficient, a small fraction of the wall is covered with an AFSS and the rest of the wall is metallized. Typically a 30 cm x 30 cm AFSS will give sufficient control into a small room 4 m x 4 m, further panels would be required for larger areas. The metallized area prevents any signal from penetrating into the wall material and passing through it, no matter what the signal frequency is as the incoming wave is almost totally reflected. Alternatively, the AFSS areas form the windows with controlled transparency.

The paper is organised as follows. The operational principle of the proposed bi-state AFSS structures capable of switching between the transparency and reflectance states is illustrated first for the case of a single polarisation operation in Section II. The dual polarised intertwined AFSSs, analysed by full-wave (FW) simulations in CST Microwave Studio (MWS) [21], the details of the *pin* diode switching circuitry and the distribution of the dc control signals are discussed in Sections III and IV for the double and single-layered arrays, respectively. In Section V the AFSS performance is validated experimentally and the measurement results are discussed in comparison with the predictions of numerical simulations. The main features of the AFSSs comprised of the periodic arrays of interwoven slots are summarised in the Conclusion.

## II. SINGLE POLARISED BI-STATE INTERWOVEN SPIRAL SLOT ARRAY WITH SEPARATE SWITCHING LAYER

The unit cell layout of a sample two layer AFSS providing a bi-state response at a single polarization of the incident field is shown in Fig. 1. In this arrangement, briefly outlined in [22], a periodic array of intertwined bifilar spiral slots is combined with a bi-state switchable dipole array deployed on the opposite side of a thin dielectric substrate. The ends of adjacent strip dipoles are interconnected by *pin* diodes to form columns or rows, and the biasing voltage is applied at the array periphery, as in a basic active bi-state dipole array [9]-[11]. On the opposite side of the dielectric substrate, the bifilar spiral slot

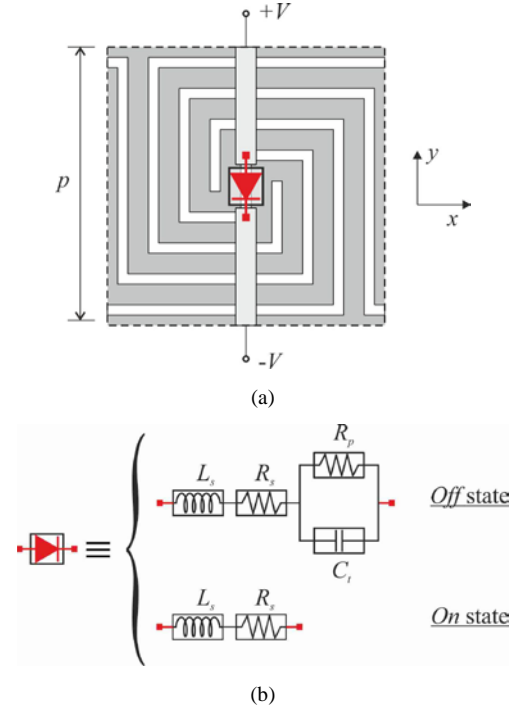


Fig. 1. (a) Unit cell of a two-layer bi-state interwoven 5-fold bifilar spiral slot elements with the switchable strip dipoles in the foreground (view from the back). One *pin* diode per unit cell is connected between the ends of dipoles. Geometrical parameters of the square unit cell: lattice period  $p = 5.4$  mm, spiral pitch 2.4 mm, slot width  $s = 0.2$  mm and thickness  $17.5 \mu\text{m}$ . Separation between the free-standing conductor patterns is 0.4 mm. (b) Equivalent circuits of diodes in the forward (*on*) and reverse (*off*) bias states.

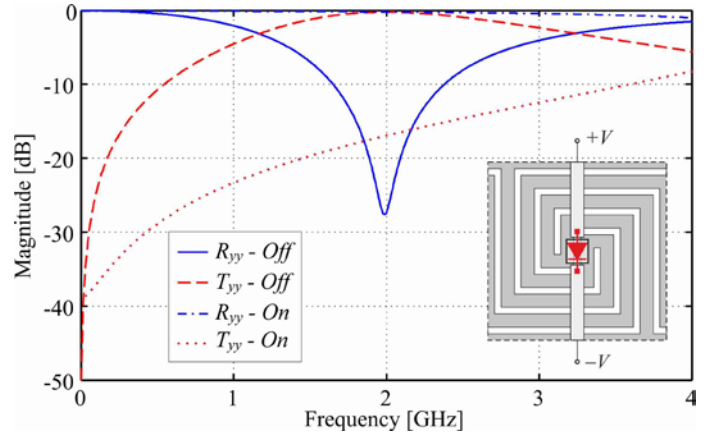


Fig. 2. Simulated transmittance and reflectance of the AFSS with the unit cell from Fig. 1 at normal incidence of a y-polarized wave when *pin* diodes are in the *off* (solid and dashed lines) and *on* (dash-dotted and dotted lines) states. In the simulations the circuit parameters are:  $R_s = 2.1 \Omega$ ,  $L_s = 0.6$  nH, and  $C_t = 0.17$  pF, see datasheets of Infineon diodes BAR64-02V-SC79 [23].

arms, protruding from adjacent unit cells into the conductor between the turns of the primary spiral slot in a reference unit cell, are intertwined either column- or row-wise depending on the parity (odd or even number) of spiral folds. Such stacked arrays exhibit a passband response to one of the incident field polarisations, whereas they are practically opaque for the orthogonal polarisation; their resonance has broad FBW at grossly subwavelength unit cell size  $p \ll \lambda$ , similarly to the

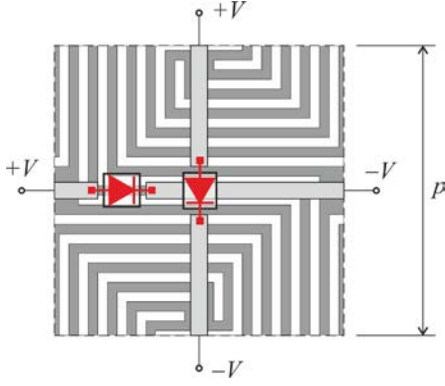


Fig. 3. Unit cell layout of a bi-state two layer interwoven 4-fold quadrifilar spiral slot AFSS with switching cross dipoles in a separate layer (view from the back). Two *pin* diodes per unit cell are connected between the arms of adjacent cross dipoles. Geometrical parameters of the unit cell: lattice period  $p = 6$  mm, spiral pitch 1.6 mm, spiral conductor width  $s = 0.2$  mm and thickness 35  $\mu\text{m}$ . Width of cross dipoles is 0.35 mm. The two conductor patterns are printed on 0.8-mm-thick dielectric substrate with permittivity  $\epsilon_r = 2.2 - j0.0009$ .

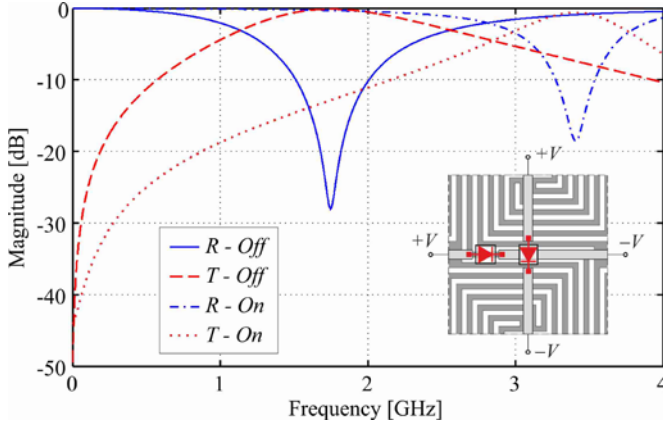


Fig. 4. Transmittance and reflectance at normal incidence of the AFSS of Fig. 3 when *pin* diodes are in the *off* (solid and dashed lines) and *on* (dash-dotted and dotted lines) states. In the simulations the circuit parameters are:  $R_s = 2.1$   $\Omega$ ,  $L_s = 0.6$  nH, and  $C_t = 0.17$  pF, see datasheets of Infineon diodes BAR64-02V-SC79 [23].

arrays of intertwined quadrifilar spiral strips [4].

The spiral slot array with the square unit cell illustrated in Fig. 1a has been simulated in CST MWS using a single unit cell with doubly periodic boundary conditions. The diodes are modelled using their simplified equivalent circuits for the forward and reverse biased states [15], as depicted in Fig. 1b. At the forward bias (*on* state), the diode presents a resistance  $R_s$  in series with the packaging inductance  $L_s$ . At the reverse bias (*off* state), the circuit becomes a parallel combination of  $R_p$  and  $C_t$  in series with  $L_s$ , where  $C_t$  is a sum of the device junction and packaging capacitances; resistance  $R_p$  typically exceeds 10 k $\Omega$  and is neglected in the simulations.

The transmittance and reflectance of the AFSS simulated at normal incidence of a vertically polarized plane wave are

shown in Fig. 2 for both the *off* and *on* states of the *pin* diodes. Since the slot array is opaque for a horizontally polarised wave in the specified frequency band, irrespective of the diodes state, this case is not presented in Fig. 2.

When the biased diodes are in the *off* state, the two-layer AFSS is transparent to the illuminating wave in the vicinity of the resonance of the passive intertwined bifilar spiral slot array. In this case the strip dipoles of length  $p \ll \lambda$  resonate at a much higher frequency. Thus, the strip dipoles barely affect the subwavelength passband resonance of the slot array which has FBW<sup>1</sup>  $\sim 37\%$  at  $\lambda_r / p \sim 28$ , where  $\lambda_r$  is the resonance wavelength at frequency  $\sim 2$  GHz.

When the diodes are biased in the *on* state, the columns of the dipole array perform as continuous conducting strips which exhibit an inductive impedance and a high-pass filter response. However, given that  $p \ll \lambda_r$ , the resonance of the spiral array is significantly below the cut-off frequency of the high-pass band and the two-layer structure is strongly reflective.

### III. DUAL POLARISED BI-STATE INTERWOVEN SPIRAL SLOT FSS WITH SEPARATE SWITCHING LAYER

The concept of using dedicated strip arrays to control the response of the singly polarized interwoven spiral AFSSs described in the previous section can be extended to the dual polarization regime. To this aim, it is possible to combine an interwoven quadrifilar spiral slot array and a strip mesh with embedded *pin* diodes, which bridge the gaps in both horizontal and vertical strips of the biasing and switching circuit. Making use of SMT components, *pin* diodes can be deployed without touching the crossing strips. Then the biasing voltages are supplied independently to the columns and rows of the array, as shown in Fig. 3. The widths of the strip conductors and the gaps across them are dictated by the footprint and package size of actual *pin* diodes used in the AFSS.

The simulated transmittance and reflectance at normal incidence of the AFSS with the unit cell of Fig. 3 are displayed in Fig. 4 for both the forward (*on*) and reverse (*off*) bias states of the *pin* diodes. Similar to the singly polarized AFSS with the diodes in the *off* state, the 2D grid of the crossed dipoles is almost transparent to the incoming wave near the resonance of the passive FSS of interwoven quadrifilar spiral slots. This happens because the latter array resonates at a much lower frequency than the crossed dipoles, whose resonance frequency is decreased to a relatively small extent only by the *off* state capacitance of *pin* diodes. Therefore, the dipole array has negligible effect on the passband response of the spiral slot array. When the diodes are switched in the *on* state, the rows or columns of the 2D grid behave as continuous conducting strips, which present an inductive impedance and act as a high-pass filter. But due to the unit cell subwavelength size, the filter passband is considerably higher than the AFSS operational frequency, which results in a strongly reflective response. Dual polarization operation is accomplished by applying bias to both

<sup>1</sup> FBW is defined as the transmission bandwidth at the reflectance level  $|R| = -10$  dB normalized to the resonance frequency  $f_r$ .



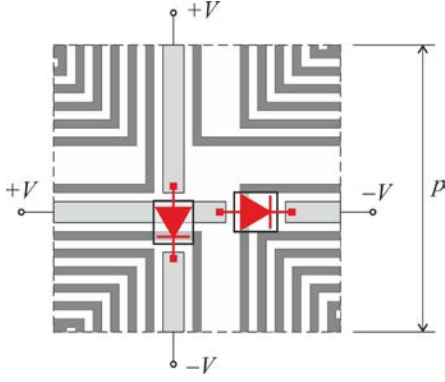


Fig. 5. Unit cell layout of a bi-state single-layer interwoven 11-fold Brigid's cross slot AFSS with switchable cross dipoles interspersed between the central vertical and horizontal conductors of the resonant elements. Two *pin* diodes per unit cell are connected between the arms of adjacent cross dipoles. Geometrical parameters of the unit cell: lattice period  $p = 8.2$  mm, conductor width  $s = 0.25$  mm and thickness  $35$   $\mu\text{m}$ . Width of cross dipoles is  $0.6$  mm. The two conductor patterns are printed on  $0.8$ -mm-thick dielectric substrate with permittivity  $\epsilon_r = 2.2 - j0.0009$ .

the vertical and horizontal dipole strips.

#### IV. SINGLE-LAYER DUAL POLARISED BI-STATE INTERWOVEN SLOT FSS WITH INTEGRATED SWITCHING CIRCUIT

The principles of realizing the bi-state AFSSs with integrated bias circuitry described in the previous sections can be applied to interleaved array configurations with all the conductors

deployed on the same surface. The doubly periodic arrays of intertwined Brigid's crosses, cf. e.g. [17], [18], are particularly suitable for this purpose. They exhibit broader FBW than the interwoven quadrifilar spiral arrays with the same periodicity but have slightly higher resonance frequencies [17], [18]. In contrast to the AFSS composed of the interwoven quadrifilar spiral slot arrays, where the strip grid with diodes must be placed in a separate layer, the canonical configuration of complementary intertwined Brigid's crosses allows the strip dipoles to be interspersed in the slots to accomplish a single layer dual polarised bi-state AFSS with integrated bias circuitry.

The unit cell layout of the complementary Brigid's cross AFSS depicted in Fig. 5 has been designed for a resonance frequency of about  $2$  GHz. As apparent, the slot between conductors at the centre of the unit cell is widened to accommodate the strip dipoles, whose width is dictated only by the dimensions of commercially available *pin* diodes (Infineon diodes BAR64-03W with the larger package SOD323 [23] have been used in this example). The SMT type *pin* diodes bridge the gaps between strip dipoles in the grid and jump over the crossing arms of Brigid's crosses. The biasing voltage applied at the grid periphery enables independent control of the array columns and rows and the dual polarized operation of such a single-layer AFSS.

The AFSS with the unit cell layout of Fig. 5 has been simulated in CST MWS at normal and oblique incidence of TE

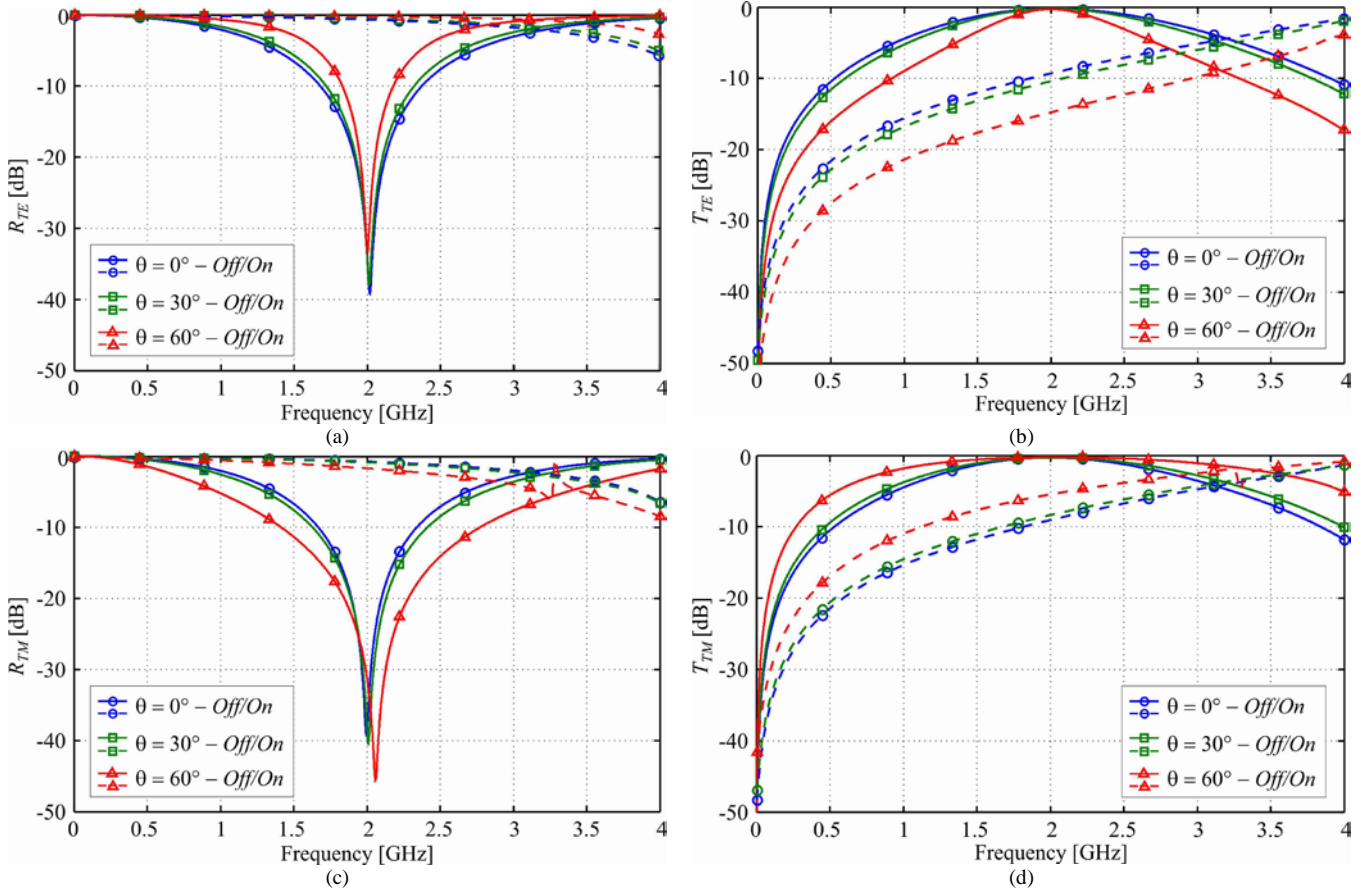


Fig. 6. Simulated reflectance and transmittance of the AFSS with the unit cell of Fig. 5 at normal and oblique incidences of (a)-(b) TE and (c)-(d) TM waves when the *pin* diode switches are in the *off* (solid lines) and *on* (dashed lines) states. The diode parameters are:  $R_s = 2.1$  Ohm,  $L_s = 0.6$  nH, and  $C_i = 0.17$  pF, see datasheet of Infineon diodes BAR64-03W-SOD323 [23].

and TM plane waves with the diodes in both the *on* and *off* states. The diode models were incorporated in the EM analysis using the equivalent circuits of the diode forward and reverse bias states shown in Fig. 1(b). The simulated AFSS responses shown in Fig. 6 demonstrate that similarly to the interwoven spiral slot array described in the previous section, the AFSS with the diodes in the *off* state is practically transparent at either polarization of the incident field near the resonance frequency of the passive intertwined Brigid's cross slot array. When the diodes are switched *on*, the columns and rows of the strip dipoles form continuous conductor strips isolated at their crossings. Such a mesh behaves as a high-pass filter and exhibits a substantially reflective isotropic response like that in the two-layer AFSS.

The reflectance and transmittance characteristics displayed in Fig. 6 at variable incidence angles of TE and TM waves for both the *off* and *on* states of the switchable diodes demonstrate that in the *off* state the AFSS exhibits high stability of the resonance frequency in a broad range of incidence angles at both TE and TM wave polarisations. The response remains fairly stable also in the *on* state. When the diodes are switched to the *off* state, the AFSS is transparent to both TE and TM polarised waves near the resonance of the passive intertwined Brigid's cross slot array. The opaqueness of the surface in the *on* state slightly decreases at larger incidence angles of TM polarised waves, whereas it improves for obliquely incident TE polarised waves, which is consistent with the reflectance trend at oblique incidence of strip arrays [24].

Comparison of the responses of the single- and two-layer AFSSs show that the two-layer FSS exhibits a higher packaging density  $p/\lambda_r$ , or equivalently a slightly lower resonance frequency for a given unit cell size, while the FBW remains nearly the same. A smaller electrical size of the unit cell also entails higher opaqueness of the AFSS in the diodes *on* state due to the progressive broadening of the low-frequency rejection band in denser strip arrays.

Generally, the two-layer AFSS may offer more freedom in the switching circuitry layout, including the possibility of accommodating wider strips of the cross dipoles to attain a higher rejection in the specified frequency band without sacrificing the packing density,  $p/\lambda_r$ , and the performance figure of merit. However, slightly lower performance of the single-layer AFSSs may be counterbalanced by the ease and low cost of their fabrication. Besides, the additional constraints imposed by the interspersed grid of strip dipoles into the single-layer AFSS can be somewhat alleviated by adopting narrower dipoles and gaps, and diodes with a smaller package<sup>2</sup>. For example, the use of the same diodes as in the two-layer AFSS described in Section III would result in a smaller unit cell of the single-layer AFSS and improved performance in both modes of operation.

<sup>2</sup> The larger packaged diodes have been purposely employed in the single-layer design to make it compatible with the low cost conductive inkjet printing and assess this technology in comparison with the standard photolithography.

## V. EXPERIMENTAL VERIFICATION

The proposed concept of AFSSs based on the complementary layout of the interwoven spiral and Brigid's cross arrays has been validated experimentally. The AFSS prototypes were manufactured by both photolithography and conductive inkjet printing. The AFSSs fabricated by the two methods have performed similarly, albeit the prototypes with inkjet printed conductors exhibited slightly higher losses of extra 1 dB. Therefore, the measurement results are presented here only for the AFSS specimens fabricated by photolithography.

### A. Measurement setup

The fabricated AFSSs have been characterized by both transmission and reflection measurements. The measurement setup is shown schematically in Fig. 7. For the transmission measurements, the specimens were fitted in a metallic frame placed between two Rohde and Schwarz HF906 wideband horns, connected to an HP8510C vector network analyser (VNA). The diffraction by the frame window was calibrated out first by characterizing the fixture without samples. Parasitic reflections were undetectable in these tests.

For reflectivity measurements, the same wide band horns were attached to a NRL (Naval Research Laboratory) arch [25], housed inside an anechoic chamber. The specimens were placed on a low density polystyrene supporting structure, surrounded by pyramidal absorbers. The setup was calibrated without a sample and with a metal plate put in place of the sample. The measurement accuracy was enhanced by time gating to separate the array response from the spurious back scattering caused by multipath propagation.

### B. Bi-layer Interwoven Spiral Slot AFSS

The manufactured prototype of the AFSS described in Section III, made by the complementary array of interwoven quadrifilar spirals combined with a conductor strip grid acting

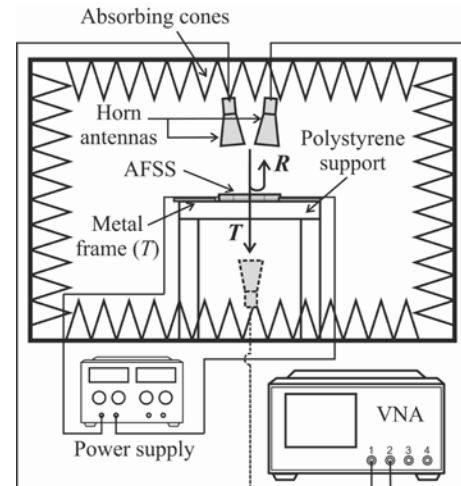


Fig. 7. Schematic illustration of the reflection ( $R$ ) and transmission ( $T$ ) measurement setups. Two horn antennas were used for each measurement, either on the same side or the opposite sides of the AFSS for  $R$  and  $T$  measurements, respectively.

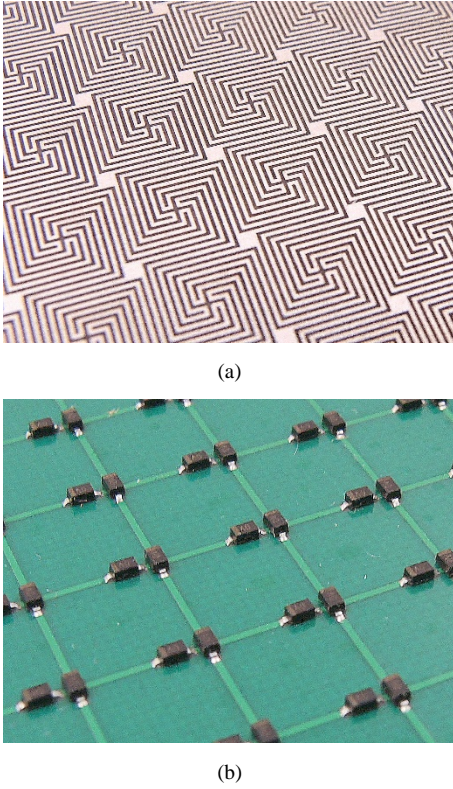


Fig. 8. A section of the bi-layer FSS prototype: (a) surface of the resonant interwoven spiral slot array; (b) the conductor strip grid with integrated *pin* diode switches. The two conductor patterns are printed on 0.8-mm-thick dielectric substrate with permittivity  $\epsilon_r = 2.2 - j0.0009$  (Taconic TLY5).

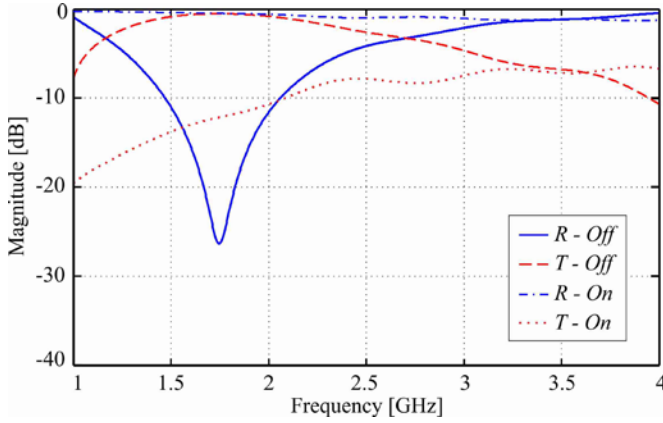


Fig. 9. Reflectance and transmittance of the AFSS shown in Fig. 8 measured at normal incidence with *pin* diode switches in the *off* (solid and dashed lines) and *on* (dash-dotted and dotted lines) states.

as the switching and biasing circuit, comprised of  $49 \times 49$  square unit cells of size  $p = 6$  mm, printed on a square  $298.7 \times 298.7$  mm<sup>2</sup> substrate of thickness 0.8 mm with nominal relative permittivity  $\epsilon_r = 2.2 - j0.0009$  (Taconic TLY5). The periodic array of interwoven quadrifilar spiral slots and the dipole grid providing bias to the diodes were printed on the opposite sides of the dielectric substrate. This prototype required the use of 4802 Infineon *pin* diodes of type BAR64-02V for surface mount with package SC79 [23]. The top and bottom sides of the AFSS panel, containing the array of interwoven quadrifilar

spiral slots and the strip mesh with the *pin* diode switches, are shown in Fig. 8(a) and 8(b), respectively.

The AFSS response was measured in both the *on* and *off* states of the *pin* diodes. To switch the *pin* diodes into the *on* state, a forward bias voltage of  $\sim 34$  V was applied at the periphery of the FSS panel in the measurement of both transmission and reflection. In this AFSS the biasing and switching grid actually consists of two orthogonal linear bi-state dipole arrays [9]–[11]. Adjacent dipoles bridged by SMT *pin* diodes form the grid rows and columns that are connected in parallel to two pairs of vertical and horizontal bias buses to which the biasing voltages can be separately applied at the array periphery. This structure results in a mixed series-parallel electrical configuration for the biasing of the diodes. For forward bias, the power supply delivered a current of  $\sim 34.5$  mA, which is distributed among the rows (or columns) of diodes supplying each a bias current of  $\sim 0.7$  mA. The FSS attenuation was not affected by further increments of the current. For the case of reverse bias, the power supply was simply disconnected and no voltage applied to the array.

Fig. 9 shows the transmittance and reflectance of the AFSS of Fig. 8 for a normally incident wave measured in both the *on* and *off* states of the *pin* diodes. It can be seen that with the diodes in the *off* state the structure is nearly transparent, the small losses of  $\sim 1$  dB being due to the diode resistance at the resonance of the intertwined spiral slot array. In this case, the resonance of the dipole array occurs at a frequency much higher than that of the spiral slot array at  $f_r \approx 1.75$  GHz. The measured FBW at the reflectance level of  $-10$  dB is  $\sim 34\%$ , and both the  $f_r$  and FBW are well correlated with simulation results in Fig. 4. When the diodes are in the *on* state, the rows or columns of the horizontal or vertical dipole array behave as continuous metal strips and produce a high-pass filter response. Because of the substantially subwavelength unit cell size, the resonance frequency of the intertwined spiral slot array is considerably below the high-pass band, and the overall response of the AFSS is strongly reflective. These characteristics are in good agreement with those predicted by the FW simulations in CST MWS displayed in Fig. 4.

### C. Single-layer Intertwined Brigid's Cross Slot AFSS

The prototype of the single layer bi-state AFSS described in Section IV is shown in Fig. 10. It is made of a complementary intertwined Brigid's cross array interspersed by the conductor strip grid acting as the switching and biasing circuit. The array comprised of  $33 \times 33$  square unit cells of size  $p = 8.2$  mm each was fabricated on a  $275.8 \times 275.8$  mm<sup>2</sup> wide and 0.8-mm-thick substrate with nominal relative permittivity  $\epsilon_r = 2.2 - j0.0009$  (Taconic TLY5). As in the first AFSS prototype, the biasing and switching grid with embedded *pin* diodes is formed by two orthogonal bi-state dipole arrays [9]–[11] insulated at their crossing points by the diode packaging. Two Infineon diodes of type BAR64-03W with SMT package SOD323 [23] were soldered in each unit cell, with a total of 2178 diodes used in this prototype.

In both the measurements of transmission and reflection, a forward voltage of  $\sim 23$  V was supplied to flip the *pin* diodes from the *off* to the *on* state. A mixed series-parallel bias



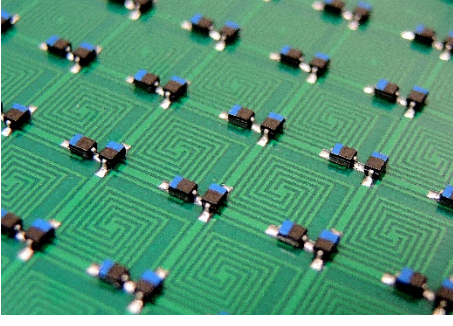


Fig. 10. A section of the single-layer bi-state AFSS prototype based on the complementary array of intertwined Brigid's crosses paired to a conductor strip grid with surface mounted *pin* diode switches and biasing circuit interspersed between the resonant FSS conductors. The FSS is printed on 0.8-mm-thick dielectric substrate with permittivity  $\epsilon_r = 2.2 - j0.0009$ .

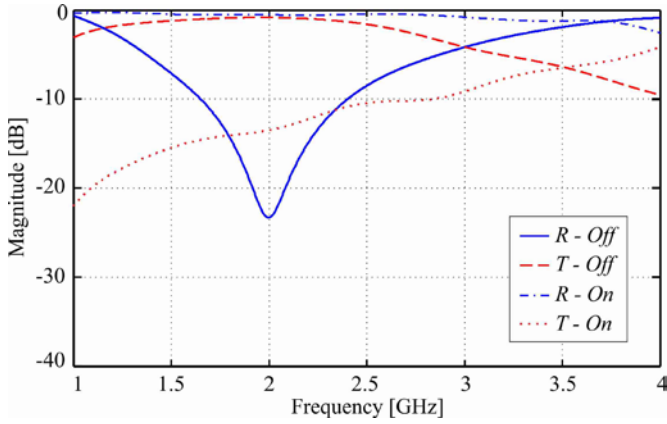


Fig. 11. Reflectance and transmittance of the FSS panel shown in Fig. 10 measured at normal incidence with *pin* diode switches in the *off* (solid and dashed lines) and *on* (dash-dotted and dotted lines) states.

distribution network was realized by adjacent collinear dipoles interconnected by *pin* diodes to form rows and columns that are attached in parallel to two pairs of vertical and horizontal bias buses running along the array periphery. For forward bias, the power supply delivered a current of  $\sim 22.5$  mA, which was distributed across the columns (or rows) of diodes giving each a bias current  $\sim 0.7$  mA. Further increase of the bias current had no discernible effect on the attenuation. In the case of reverse bias, no voltage was applied.

The measured transmittance and reflectance of the AFSS illuminated at normal incidence are shown in Fig. 11 for both the *on* and *off* states of the *pin* diodes. It appears that the AFSS is practically transparent when the diodes are in the *off* state and exhibit small losses of  $\sim 1$  dB near the resonance of the intertwined Brigid's cross slot array, as predicted by CST MWS simulations. Indeed, as discussed in Section IV, the dipole array resonance is at a much higher frequency, in spite of the effect of the parasitic *off* state capacitance of *pin* diodes. Therefore, the dipoles weakly affect the passband resonant response of Brigid's cross array at  $f_r \approx 2.1$  GHz with the FBW measured at the level of  $-10$  dB being  $\sim 43\%$ . When the diodes are in the *on* state, the AFSS becomes strongly reflective because columns or rows of the vertical or horizontal dipoles behave as continuous conducting strips providing a high-pass filter

response with the cut-off frequency much higher than the resonance frequency of the Brigid's cross array. The measured transmission and reflection characteristics at normal incidence, shown in Fig. 11, demonstrate good agreement with the FW simulations of the corresponding infinite array modelled in CST MWS using a single unit cell and periodic boundary conditions.

The response of the single-layer AFSS prototype shown in Fig. 10 has been measured at oblique incidence of TE and TM waves. The transmission characteristics measured at incidence angles of  $0^\circ$ ,  $30^\circ$ , and  $60^\circ$  are shown in Fig. 13 at the *pin* diode switches in both the *off* (solid lines) and *on* (dashed lines) states. Transmission losses when the AFSS operates in the *on* state of switches are in the range 0.6-1.2 dB. The measured characteristics agree very well with the FW simulation results shown earlier in Fig. 6, especially when the diodes are in the *off* state. When the diodes are in the *on* state, the measured responses of the AFSS exhibit the same trends of the incidence angle dependences of both TE and TM polarizations as in FW simulations, but attain higher isolation. The latter is attributed to higher losses of the diode switches and their solder joints, which are not fully described by the nominal resistance of the diode models in the FW simulations. Thus, in this AFSS

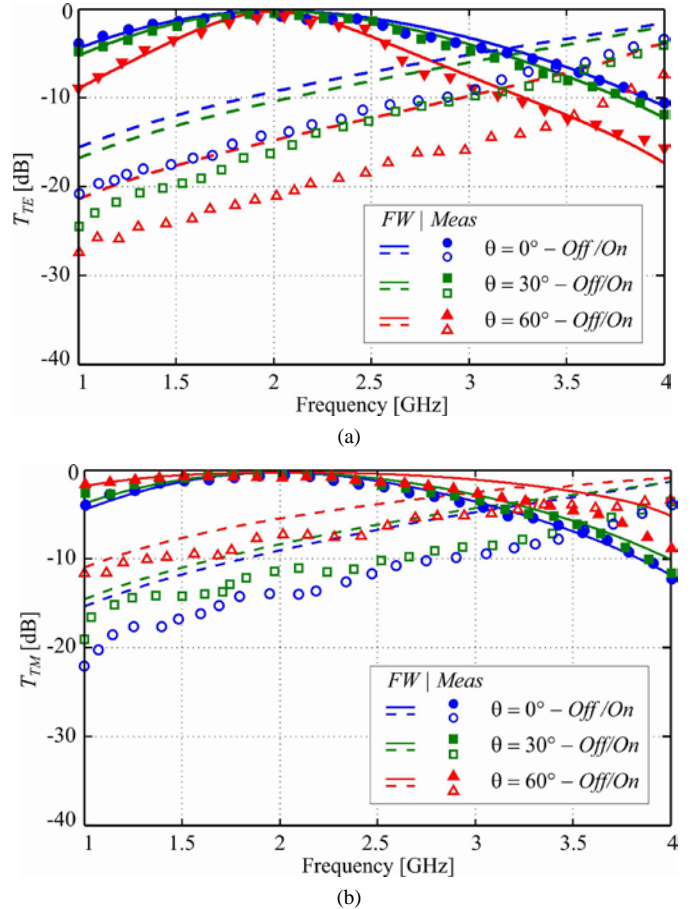


Fig. 12. Measured transmittance of the AFSS panel shown in Fig. 10 at normal and oblique incidence of (a) TE and (b) TM waves when the *pin* diode switches are in the *off* (solid lines) and *on* (dashed lines) states. Measured data (square, circle, and triangle markers for  $0^\circ$ ,  $30^\circ$ , and  $60^\circ$  incidence, respectively, filled and empty for the *off* and *on* states) are juxtaposed with the corresponding simulated results from Fig. 6 (solid and dashed lines).

arrangement, the real switches with higher losses turn out to improve the AFSS *on/off* performance, rather than degrade it.

## VI. CONCLUSION

A novel class of AFSSs with substantially subwavelength unit cells and integrated biasing wiring has been developed and tested. The presented AFSS arrangements are composed of the periodic complementary arrays of planar interwoven spirals and Brigid's crosses with the slots spirally wound and intertwined in adjacent unit cells. The key idea is to purposely leverage the subwavelength unit cell size of the patterned conductor screens with such convoluted and interwoven slot layouts and combine them with the grids of voltage controlled dipoles with integrated *pin* diodes located either on the same or opposite sides of a thin dielectric substrate. The substantially subwavelength size of the array unit cell ensures that the dipoles resonate far away from the array operational frequency and thus weakly interfere when the switches are in the *off* state. Then only the interwoven slot array determines the AFSS response. Conversely, in the *on* state of the switches, the grid of continuous strips formed by the interconnected dipoles enables a high isolation response of the AFSS - in fact, the smaller the unit cell size, the higher the isolation. As a result, bi-state transparency and reflectance at specified frequencies are achieved by the AFSS. The grid of dipoles allows switching of columns and rows of diodes separately, thus enabling independent control of the AFSS transparency for the vertically and horizontally polarized incident waves. It is important to stress here that the state of the *pin* diodes is controlled for the whole AFSS by voltage applied to the array periphery only but not to individual switches.

The presented AFSS arrangements maintain all the merits of the arrays with substantially subwavelength unit cells inherent to the passive interwoven arrays. At the same time, they are substantially immune to the effects of switch parasitics, particularly, the performance degradation caused by the reverse bias capacitance of real switches. Additionally, the insertion loss of diodes in the *on* state actually improves the array isolation, rather than degrades its performance. The simulation and measurement results show that the proposed AFSSs with integrated switching and biasing circuitry achieve isolation of ~15 dB between the transparency and reflectance regimes. This rate of isolation reduces the separation required for frequency reuse by a factor more than 3, which can significantly improve spectrum efficiency [26].

Power consumption and efficiency represent an important aspect of the AFSS design. A smaller unit cell size dictates the need for more *pin* diodes for an aperture of a given size. However, this does not directly imply a reduction of power efficiency. On the one hand, in the considered operational regimes, power is applied only in the *on* state of *pin* diodes, and moreover power consumption in voltage controlled switches is normally low. On the other hand, the efficiency of a bi-state AFSS is mostly an implementation issue. In the prototypes described in Section V we used commercial low cost *pin* diode switches. Power consumption of the tested panels was about 1 W, and it could be further reduced with different types of *pin* diodes, e.g. InGaAs or InAlAs/InGaAs/InP switches or high

frequency switch ICs based on FETs. Alternatively, very low loss RF MEMS switches with very low control power can be used. The AFSS structures presented in the paper are readily adaptable to any switch technology.

All the proposed AFSS designs are compatible with the manufacturing processes based upon standard photolithography or inkjet printing and SMT component placement techniques. It is also worth emphasizing that the presented designs are fairly flexible in terms of unit cell size. We aimed at electrically small unit cells  $< 1/20$  of the wavelength at the centre frequency to achieve high angular stability and a broad operating bandwidth. But the unit cell can be made larger, with a smaller number of switches required for a given aperture size and slightly lower power consumption. But this will upset the AFSS performance. Consideration of such factors and the related trade-offs can only be addressed at the level of a specific design/application that is beyond the aim and scope of this paper.

Finally, it is important to note that the broad FBW and high angular and polarisation stability of the intertwined Brigid's cross and intertwined spiral arrays are achievable with scalable unit cell dimensions tailored to the specified operational frequencies. This enables the design and fabrication of compact AFSSs for applications in reconfigurable and controllable electromagnetic architecture of buildings using both the low-cost wet etching and inkjet printing fabrication techniques.

## VII. ACKNOWLEDGEMENT

The authors would like to thank Dr K. L. Ford, University of Sheffield, for useful advice, Michal Červený, Czech Technical University, Prague, for his help in performing the measurements, and Colin Hallam, Trackwise Ltd, for managing the accurate manufacturing of AFSS prototypes. The use of the measurement facilities of the Department of Engineering Science of the University of Oxford is also gratefully acknowledged.

## REFERENCES

- [1] F. Huang, J. C. Batchelor and E. A. Parker, "Interwoven convoluted element frequency selective surfaces with wide bandwidths," *Electron. Lett.*, vol. 42, pp. 788-790, Jul. 2006.
- [2] B. Sanz-Izquierdo, E. A. Parker, J.-B. Robertson, and J. C. Batchelor, "Singly and dual polarized convoluted frequency selective structures," *IEEE Trans. Antennas Propagat.*, vol. 58, no. 3, pp. 690-696, Mar. 2010.
- [3] A. Vallecchi and A. G. Schuchinsky, "Entwined spirals for ultra compact wideband frequency selective surfaces," *Proc. 4<sup>th</sup> European Conference on Antennas and Propagation, EuCAP 2010*, Barcelona, Spain, 12-16 Apr. 2010, A18P2-5.
- [4] A. Vallecchi and A. G. Schuchinsky, "Entwined planar spirals for artificial surfaces", *IEEE Antennas Wireless Propagat. Lett.*, vol. 9, pp. 994-997, 2010.
- [5] K. Sarabandi and N. Behdad, "A frequency selective surface with miniaturized elements," *IEEE Trans. Antennas Propag.*, vol. 55, no. 5, pp. 1239-1245, May 2007.
- [6] A. C. M. Austin, M. J. Neve, and G. B. Rowe, "Modelling propagation in multi-floor buildings using the FDTD method," *IEEE Trans. Antennas Propagat.*, 59, no. 11, pp. 4239-4246, 2011.
- [7] J. P. Turpin, J. A. Bossard, K. L. Morgan, D. H. Werner, and P. L. Werner, "Reconfigurable and tunable metamaterials: A review of the theory and applications," *International Journal of Antennas and Propagation*, vol. 2014, Article ID 429837, 18 pages, 2014. doi:10.1155/2014/429837.
- [8] T. K. Chang, R. J. Langley, E. A. Parker, "Active frequency selective surfaces," *IEE Proc. Microw. Antennas Propagat.*, vol. 143, no. 1, pp. 62-66, Feb. 1996.



- [9] B. M. Cahill and E. A. Parker, "Field switching in an enclosure with active FSS screen," *Electron. Lett.*, vol. 37, no. 4, pp. 244–245, Feb. 15, 2001.
- [10] A. Tennant and B. Chambers, "A single-layer tuneable microwave absorber using an active FSS," *IEEE Microw. Wireless Compon. Lett.*, vol. 14, no. 1, pp. 46–47, Jan. 2004.
- [11] P. Edenhofer and A. Alpaslan, "Active frequency selective surfaces for antenna applications electronically to control phase distribution and reflective/transmissive amplification," in *Proc. IEEE/ACES Int. Conf. on Wireless Communications and Applied Computational Electromagnetics*, Apr. 3–7, 2005, pp. 237–240.
- [12] G. I. Kiani, K. L. Ford, L. G. Olsson, K. P. Esselle, and C. J. Panagamuwa, "Switchable frequency selective surface for reconfigurable electromagnetic architecture of buildings," *IEEE Trans. Antennas Propag.*, vol. 58, no. 2, pp. 581–584, Feb. 2010.
- [13] P. S. Taylor, E. A. Parker, and J. C. Batchelor, "An active annular ring frequency selective Surface," *IEEE Trans. Antennas Propag.*, vol. 59, no. 9, pp. 3265–3271, Sept. 2011.
- [14] K. ElMahgoub, F. Yang, and A. Z. Elsherbeni, "Design of novel reconfigurable frequency selective surfaces with two control techniques," *Progress In Electromagnetics Research C*, vol. 35, 135–145, 2013.
- [15] A. Vallecchi, R. J. Langley, and A. G. Schuchinsky, "Active singly and dual polarised interwoven spiral frequency selective surfaces", in *Proc. EuCAP 2014*, The Hague, The Netherlands, 6–11 Apr. 2014.
- [16] A. Vallecchi, R. J. Langley, A. G. Schuchinsky, "Voltage controlled intertwined spiral arrays for reconfigurable metasurfaces," *Int. Journal of Antennas and Propagation*, 171637, 2014.
- [17] A. Vallecchi and A. G. Schuchinsky, "Metasurfaces with intertwined conductor patterns," *Proceedings of Metamaterials' 2011*, Barcelona, Spain, 10–15 October 2011.
- [18] A. Vallecchi, R. J. Langley, and A. G. Schuchinsky, "Metasurfaces with interleaved conductors: Phenomenology and applications to frequency selective and high impedance surfaces," *IEEE Trans. Antennas Propag.*, vol. 64, no. 2, pp. 599–608, Feb. 2016.
- [19] L. Subrt, D. Grace, and P. Pechac, "Controlling the Short - Range Propagation Environment Using Active Frequency Selective Surfaces," *Radioengineering*. 2010, vol. 19, no. 4, pp. 610 - 615, 2010.
- [20] L. Subrt, L. P. Pechac, L. Ford, R. Langley, J. Rigelsford, "Controlling coverage for indoor wireless networks using Metalized Active FSS Walls", 19th Asia-Pacific Conference on Communications (APCC), 2013
- [21] "CST - Computer Simulation Technology". <https://www.cst.com/>, accessed January 2016.
- [22] A. Vallecchi, R. J. Langley and A. G. Schuchinsky, "Reconfigurable frequency selective surfaces with interleaved spiral slots," in *Proc. 2014 IEEE Antennas Propagat. Soc. Int. Symp.*, Memphis, TN, 2014, pp. 2098–2099.
- [23] [http://www.infineon.com/dgdl/Infineon-BAR64series-DS-v01\\_02-EN.pdf?fileId=5546d4625607bd130156121f289c38b5](http://www.infineon.com/dgdl/Infineon-BAR64series-DS-v01_02-EN.pdf?fileId=5546d4625607bd130156121f289c38b5)
- [24] V. V. Yatsenko, S. A. Tretyakov, S. I. Maslovski and A. A. Sochava, "Higher order impedance boundary conditions for sparse wire grids," *IEEE Trans. Antennas Propag.*, vol. 48, no. 5, pp. 720–727, May 2000.
- [25] F. C. Smith, B. Chambers, and J. C. Bennett, "Calibration techniques for free space reflection coefficients measurements," *Proc. Inst. Elect. Eng.*, vol. 139, no. 5, pp. 247–253, Sep. 1992.
- [26] E. A. Parker, J.-B. Robertson, B. Sanz-Izquierdo, J. C. Batchelor, "Minimal size FSS for long wavelength operation," *Electron. Lett.*, vol. 44, no. 6, pp. 394–395, 2008.